ACTA ABP BIOCHIMICA POLONICA

Vol. 63, No 1/2016
117–125
http://dx.doi.org/10.18388/abp.2015_1074

Regular paper

Cloning, expression, and biochemical characterization of a cold-active GDSL-esterase of a *Pseudomonas* sp. S9 isolated from Spitsbergen island soil

Monika Wicka, Marta Wanarska, Ewelina Krajewska, Anna Pawlak-Szukalska, Józef Kur and Hubert Cieśliński✉

Department of Molecular Biotechnology and Microbiology, Gdańsk University of Technology, Gdańsk, Poland

An *estS9* gene, encoding an esterase of the psychrotolerant bacterium *Pseudomonas* sp. S9 was cloned and sequenced. The deduced sequence revealed a protein of 636 amino acid residues with a molecular mass of 69 kDa. Further amino acid sequence analysis revealed that the EstS9 enzyme contained a G-D-S-L motif centered at a catalytic serine, an N-terminal catalytic domain and a C-terminal autotransporter domain. Two recombinant *E. coli* strains for production of EstS9N (a two domain enzyme) and EstS9Δ (a one domain enzyme) proteins were constructed, respectively. Both recombinant proteins were successfully produced as inclusion bodies and then purified under denaturing conditions. However, because of the low enzymatic activity of the refolded EstS9Δ protein, only the EstS9N protein was further characterized. The purified and refolded EstS9N protein was active towards short-chain *p*-nitrophenyl esters (C2–C8), with optimal activity for the butyrate (C4) ester. With *p*-nitrophenyl butyrate as the substrate, the enzyme displayed optimal activity at 35°C and pH 9.0. Additionally, the EstS9N esterase retained ~90% of its activity from 25–40°C and ~40% of its activity at 10°C. Moreover, analysis of its kinetic parameters (K_m, k_{cat}, k_{cat}/K_m) toward *p*-nitrophenyl butyrate determined at 15°C and 25°C confirmed that the EstS9 enzyme is cold-adapted. To the best of our knowledge, EstS9 is the third characterized cold-active GDSL-esterase and the first one confirmed to contain an autotransporter domain characteristic for enzymes secreted by the type V secretion system.

Key words: GDSL-family, cold-active, esterase, autotransporter, *Pseudomonas* sp. S9

Received: 01 June, 2015; revised: 28 June, 2015; accepted: 22 November, 2015; available on-line: 28 January, 2016

INTRODUCTION

Lipolytic enzymes comprising carboxylesterases (EC 3.1.1.1), phospholipases (EC 3.1.1.2) and lipases (EC 3.1.1.3) are α/β hydrolases that catalyze the hydrolysis and synthesis of acylglycerides and other fatty acid esters. Many of them do not require cofactors and have regio- and stereo-selectivity (Arpigny & Jaeger, 1999). They have also broad substrate specificity, and can exhibit organic solvent-stable catalytic activities. Hence, among this group of enzymes, carboxylesterases (EC 3.1.1.1) and lipases (EC 3.1.1.3) are important industrial enzymes with numerous applications in biotechnology (Fojan *et al.*, 2000).

Cold-active enzymes have received increasing attention because of their relevance to the development of new industrial applications in various fields of biotechnology. This group of enzymes, in contrast to mesophilic and thermophilic enzymes, is characterized by high catalytic efficiency at low temperatures (0–10°C) and usually rapid inactivation at temperatures above the enzymatic activity optimum (30 to 40°C). Therefore, use of cold-active enzymes in industrial processes can prevent the loss of thermosensitive substrates and products. However, the main advantage of use of these enzymes in industry can be the reduction of heat consumption in bioreactors. Furthermore, if necessary, after use, most of cold-active enzymes can be easily inactivated by a relatively slight elevation in temperature. Moreover, in the food industry, the use of cold active enzymes for low-temperature processes can reduce the risk of contamination by mesophilic microorganisms and eliminate undesired changes in the taste and nutritional values of the foodstuffs (Cavicchioli *et al.*, 2011).

Thus, cold-active lipases and esterases may be used as additives in food processes (e.g. cheese manufacturing, baking) (Esteban-Torres *et al.*, 2014), additives in laundry detergents (cold washing), and as biocatalysts for the organic syntheses of thermolabile compounds at low temperatures (Kulakova *et al.*, 2004). Moreover, cold-active lipolytic enzymes can be also used for bioremediation of polluted soils and wastewaters, at low and moderate temperatures (Novototskaya-Vlasova *et al.*, 2012).

This study focuses on the characterization of a cold-active EstS9 esterase from the psychrotolerant bacterium *Pseudomonas* sp. strain S9. In contrast to most well characterized cold-active esterases containing a conserved **G**-X-**S**-X-**G** consensus sequence centered around the catalytic serine (Suzuki *et al.*, 2002; Kulakova *et al.*, 2004; Soror *et al.*, 2007; Heath *et al.*, 2009; Fu *et al.*, 2011; Kang *et al.*, 2011; Brault *et al.*, 2012; Hu *et al.*, 2012; Jiang *et al.*, 2012; Jimenez *et al.*, 2012; Novototskaya-Vlasova *et al.*, 2012; Lemak *et al.*, 2012; Abdul Salam *et al.*, 2013; Berlemont *et al.*, 2013; Fu *et al.*, 2013; Kim *et al.*, 2014) the EstS9 harbors another conserved sequence **G**-**D**-**S**-**L** around this catalytic residue. To the best of our knowledge, the EstS9 is the third cold-active esterase belonging to the GDSL subfamily of lipolytic enzymes

✉e-mail: hcieslin@pg.gda.pl

Abbreviations: K_m, Michaelis constant; k_{cat}, turnover number; k_{cat}/K_m, specificity constant; SDS-PAGE, sodium dodecyl sulfate polyacrylamide gel electrophoresis; DDT, dithiothreitol; EDTA, ethylenediaminetetraacetic acid; ORF, open reading frame

(Suzuki *et al.*, 2003; Cieslinski *et al.*, 2007) described to date. Moreover, analysis of the amino acid sequence of EstS9 also revealed that this enzyme is comprised of two domains: an N-terminal catalytic domain and a C-terminal autotransporter domain. Interestingly, a review of the literature did not reveal any reports on the identification and characterization of cold-active esterases with C-terminal autotransporter domains. However, we determined that a previously identified and characterized cold-active esterase, PsEst1 esterase from *Pseudomonas* sp. strain B11-1, is also comprised of an N-terminal catalytic domain (GDSL subfamily) and a C-terminal autotransporter domain. The presence of a C-terminal autotransporter domain in PsEst1 was not reported in published data (Suzuki *et al.*, 2003). Hence, the present study is the first report of the identification and characterization of a cold-active GDSL esterase containing a C-terminal autotransporter domain.

MATERIALS AND METHODS

Characterization and identification of the S9 strain. The growth properties of the S9 strain were determined in Difco Marine broth 2216 (Becton, Dickinson and Company, *abr. DM medium*). The proteolytic, lipolytic and amylolytic activities of the strain were examined at 20°C on agar solidified DM medium supplemented with skimmed milk, tributyrin, or starch, respectively.

The genus of the S9 strain was assessed on the basis of its 16S rDNA gene sequence, amplified by PCR with primers fD1 and rP2 (Weisburg *et al.*, 1991). Then, the 16S rDNA PCR product was sequenced and the resulting DNA sequence was compared with those from the Ribosomal Database Project and the NCBI database aligned using the MEGA 5.0 http://www.megasoftware.net/ website.

Genomic DNA library construction and esterase gene identification. The genomic DNA from *Pseudomonas* sp. S9 cells was isolated and purified using a Genomic Mini AX Bacteria (A&A Biotechnology, Poland) according to the protocol with one exception. The protocol step 'incubation with the lysozyme' was extended to 1 hour. Then, the genomic DNA was digested using the EcoRI endonuclease (Thermo Scientific, USA), and the resulting DNA fragments were purified by an ethanol precipitation and cloned into a pZErO-2 vector (Invitrogen, USA) which was linearized by digestion with endonuclease EcoRI and purified by Extractme DNA Clean-Up kit (Blirt S.A., Poland). The ligated DNA was transformed into *E. coli* TOP10 cells and the resulting DNA library was screened for lipolytically active clones on double layered Luria-Bertani agar plates, called LBT2. The bottom layer was supplemented with 25 μg mL^{-1} kanamycin, while the top layer contained 25 μg mL^{-1} kanamycin, 1% (v/v) tributyrin, and 0.3 mM IPTG. The kanamycin, tributyrin, and IPTG were purchased from Sigma (USA). The plates were incubated at 37°C for 24 h and then transferred to 25°C for 8 h incubation. Afterwards, the plates were screened for the presence of recombinant colonies with lipolytic activity, which was identified by their ability to form a clear halo around the colonies.

Bioinformatics analyses. Bioinformatics analyses of the DNA insert of pZErO-2/Lip1 vector, and amino acid sequences of PsEts1, EstS9, EstS9N and EstS9Δ proteins were done with a set of bioinformatics tools used in our previous study (Wierzbicka-Wos *et al.*, 2013), with one exception. The PSORT program was not used in this study. Topographic presentations of the Pfam domains for PsEts1, EstS9, EstS9N, and EstS9Δ (Fig. 1) were done with a MyDomains – Image Creator (http://prosite.expasy.org/mydomains/).

Construction of an *E. coli* TOP10/pBADestS9N strain. A PCR product, called estS9N, was amplified using the following primers: FLipS9Nco CAGTCCATGGCGCCTAATCCTTACACCCATTTCGTCG and RLipS9-Hind-His CTAGAAGCTTGAAGTCCAGCGCAACGCCTACATTAAATAC. The NcoI and HindIII restriction sites were incorporated into the forward and reverse primer sequences, respectively. The recognition sites for the restriction endonucleases are underlined and were designed to facilitate cloning. Unfortunately, because of the presence of a NcoI restriction site inside the DNA sequence coding the EstS9 esterase, a plasmid pBADestS9N was constructed in two steps as shown in Fig. 2. Finally, the recombinant pBADestS9N plasmid was transformed into *E. coli* TOP10, and the resulting recombinant *E. coli* strain produced EstS9N (pBAD expression system; Invitrogen, USA), which was composed of an N-terminal catalytic domain, AB-transporter domain, and a C-terminal His-tag domain (Fig. 1C).

Construction of an *E. coli* TOP10/pBADestS9Δ-strain. A PCR product, called estS9Δ, was amplified using the following primers: FLipS9Nco CAGTCCATGGCGCCTAATCCTTACACCCATTTCGTCG and RLipS9-shortHind-His GATC AAGCTTGCGTTGCCCTGCTTCGGTCGG. The NcoI and HindIII restriction sites were incorporated into the forward and reverse primer sequences, respectively. The recognition sites for the restriction endonucleases are underlined and were designed to facilitate cloning.

The estS9Δ PCR product was purified using an Extractme DNA Clean-Up kit (Blirt S.A., Poland), then digested with NcoI and HindIII endonucleases and purified by ethanol precipitation. The purified DNA insert was ligated to the pBAD/*Myc*-HisA expression vector (pBAD expression system; Invitrogen, USA), previously linearized with the same endonucleases. Finally, the recombinant pBADestS9Δ plasmid was transformed into *E. coli* TOP10, to yield the resulting recombinant EstS9Δ

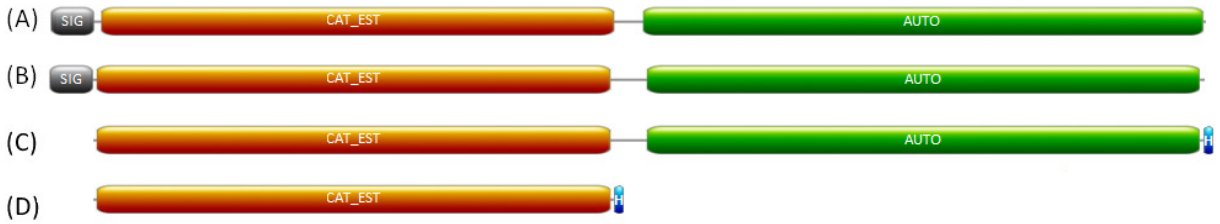

Figure 1. Topographic presentation of the Pfam domains for PsEts1 (A), EstS9 (B), EstS9N (C), and EstS9Δ (D).
SIG (grey domain), putative signal sequence; CAT_EST (orange domain), catalytic domain; AUTO (green domain), autotransporter domain; H (blue domain), His-Tag.

protein which was composed of an N-terminal catalytic domain and a C-terminal His-tag domain (Fig. 1D).

Expression and purification of the recombinant enzymes. The *E. coli* TOP10/pBADestS9N and *E. coli* TOP10/pBADestS9Δ were grown in Luria-Bertani medium (1 L) containing ampicillin (0.1 mg mL^{-1}), and incubated with agitation at 37°C to an OD_{600} of 0.5. The cultures were then supplemented with L-arabinose (0.2% w/v) to induce the expression of the *estS9N* and *estS9Δ* genes and grown for 20 h at 30°C. Next, the *E. coli* cells were harvested by centrifugation at 4°C and 4 600 × *g* for 15 min. Cell pellet was suspended in 50 mL of buffer B5 (20 mM Tris-HCl, 0.5 M NaCl, 6 M urea, 5 mM imidazole, pH 7.9), and then the *E. coli* cells were disrupted by sonication. Cell debris was collected by centrifugation at 12 800 × *g* for 20 min at 4°C, and then 50 mL of the cell-free extract was applied onto an Ni-NTA column pre-equilibrated with buffer B5. Then, the Ni-NTA column was washed out with an imidazole gradient from 5–60 mM in buffer B5. Finally, the elution step was carried out with buffer EU (20 mM Tris-HCl, 0.5 M NaCl, 6 M urea, 500 mM imidazole, pH 7.9) at a flow rate of 0.5 mL min^{-1}. For the EstS9N and EstS9Δ renaturation, the proteins in buffer EU were dialyzed against buffer R (20 mM Tris-HCl buffer, pH 7.5, containing 0.1% Triton X-100), where the concentration of urea decreased (6.0 to ~0.0 M) during dialysis (for 120 h).

The molecular weights of the denatured EstS9N and EstS9Δ proteins were estimated using SDS-PAGE (Laemmli, 1970). The protein concentration in the eluted fractions was determined by measuring the absorbance at 280 nm (BioSpectrometer Kinetic, Eppendorf, Germany).

Substrate specificity. The substrate specificity of the purified enzyme was determined at 25°C using 50 mM solutions of *p*-nitrophenyl acetate, *p*-nitrophenyl butyrate, *p*-nitrophenyl caprylate, and *p*-nitrophenyl decanoate in acetonitrile and *p*-nitrophenyl palmitate, and *p*-nitrophenyl stearate in *n*-hexane. Assays were performed by measuring the increase in absorbance at 405 nm as a result of the release of *p*-nitrophenol upon the hydrolysis of the substrates.

One unit of enzyme activity (U) was defined as the enzyme activity required for release of 1 μmol of *p*-nitrophenol from *p*-nitrophenol butyrate per minute under the above presented conditions.

Effect of temperature and pH on esterase activity. The effect of temperature on the esterase was assayed by incubating the reaction mixtures at temperatures ranging from 5 to 60°C (in 5°C increments) and measuring the activity at the same temperature with *p*-nitrophenyl butyrate at a final concentration of 3.6 mM, in 20 mM Tris-HCl buffer, pH 7.5. The enzymatic reactions were stopped after 9 min with isopropanol.

The optimum pH was determined by assaying the activity of the EstS9-His enzyme in a 10 mM Britton-Robinson buffer, with pH values ranging from 2.0 to 12.0. The enzymatic activities were quantitated at the tested pH value at 25°C with *p*-nitrophenyl butyrate. The enzymatic reactions were stopped after 9 min with isopropanol.

For the thermal stability assays, the purified enzyme was pre-incubated at 40, 50, 60, 70, 80 and 90°C in the absence of *p*-nitrophenyl butyrate. After incubating for different times (20, 40, 80, 180 and 300 min), the activity was measured by assaying the residual activities at pH 9.0, 25°C. The enzymatic reactions were stopped after 9 min with isopropanol.

For the pH stability assays, the reaction mixtures containing the appropriate substrates were incubated at 25°C and pH ranging from 5.0 to 11.0. After incubating for 20, 40 and 60 min, sample mixtures were withdrawn, and the residual enzymatic activities were measured with *p*-nitrophenyl butyrate in 20 mM Tris-HCl buffer pH 9.0 at 25°C. The enzymatic reactions were stopped after 9 min with isopropanol.

All the experiments were performed in triplicate.

Effects of selected metal ions and reagents on the enzymatic activity of EstS9N. The effects of DTT, oxidized glutathione, reduced glutathione, 2-mercaptoethanol, EDTA, and selected metal ions (Mg^{2+}, Ca^{2+}, Mn^{2+}, Ni^{2+}, Co^{2+}) at final concentrations of 5 mM, on EstS9N esterase activity were assayed in 20 mM Tris-HCl buffer, at 25°C and pH 9.0, with 3.6 mM *p*-nitrophenyl butyrate as substrate.

Sequence Accession Numbers. The *estS9* and 16S rDNA gene sequences reported in this work have been deposited in the GenBank database and assigned the accession numbers KP645181 and KP645182, respectively.

RESULTS AND DISCUSSION

Characterization and identification of the bacterial strain S9

Bacterial strain S9 was isolated from a soil sample collected in the vicinity of the Polish polar station at Isbjørnhamna in Hornsund fjord on the Spitsbergen island (77°0'0"N, 15°33'0'E). The cells of the S9 strain were Gram-negative, aerobic, non-motile and rod-shaped. On Marine broth agar, this strain formed small, round, smooth, beige colonies with a diameter of 1.5–2 mm. The optimal growth temperature for colonies was 20°C and growth was poor below 10°C and above 30°C. The strain displayed a high lipolytic activity on tributyrin agar, and a poor proteolytic activity on milk agar (growth at 20°C), respectively.

An alignment of the 16S rDNA gene sequence of the S9 strain with the appropriate sequences available in the Ribosomal Database Project and the GenBank database, demonstrated that the S9 strain should be classified as a *Pseudomonas* sp., and that its closest relatives were *Pseudomonas mandelii*, strain Asd MV-11 (GenBank:FM955880), *Pseudomonas* sp. PR3-10 (GenBank: FJ889634), *Pseudomonas* sp. SE22#2 (GenBank: AY263478) with 99% sequence identity (identities 1460/1461; gaps: 0/1461) and 100% query coverage, respectively. Interestingly, *Pseudomonas mandelii*, strain Asd MV-11, and *Pseudomonas* sp. PR3-10 were also isolated from environmental samples collected in Spitsbergen, however, *Pseudomonas* sp. SE22#2 was isolated from alpine soil. *Pseudomonas mandelii*, strain AsdMV-11, also displayed a lipolytic activity (Reddy *et al.*, 2009). However, to the best of our knowledge, identification of an enzyme(s) associated with the lipolytic activity of strain AsdMV-11 has not been isolated or characterized to date. Moreover, in contrast to strain AsdMV-11, *Pseudomonas* sp. S9 did not display an amylase activity.

Construction of a *Pseudomonas* sp. S9 genomic library and screening for clones encoding lipolytic activity

To isolate the gene encoding an enzyme with lipolytic activity, a genomic DNA library was constructed using DNA isolated from *Pseudomonas* sp. S9 and pZErO-2 vector. Next, the resulting DNA library

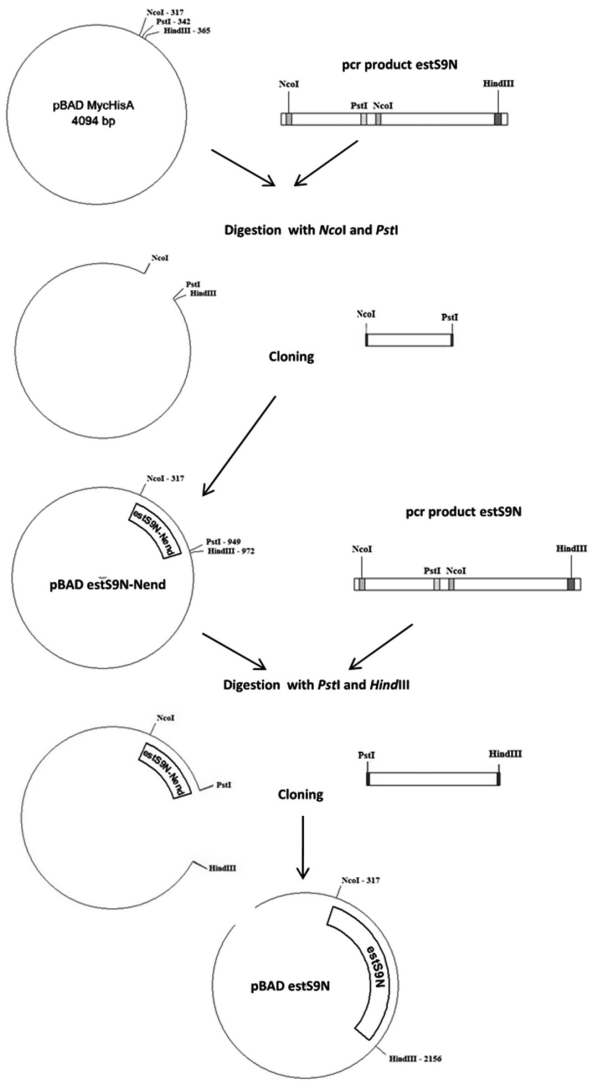

Figure 2. Construction of the pBADestS9N plasmid.

was screened for recombinant *E. coli* colonies displaying lipolytic activity towards tributyrin on LBT2 agar plates. The screening revealed one colony (named S9_Lib1) among approximately 3 000, which exhibited such lipolytic activity. The restriction analysis of pZErO-S9 Lib1, a recombinant plasmid isolated from the S9_Lib1, showed that this clone contained a *Pseudomonas* sp. S9 genomic DNA fragment of about 10 kb. Next, a series of plasmids with different fragments of the DNA insert of the pZErO-S9 Lib1 plasmid was constructed and used for transformation of *E. coli* TOP10. Finally, we found that the resulting lipolytic clones harbored the same recombinant plasmid, designated as pZErO-S9 Lib1/NotI, containing a *Pseudomonas* sp. S9 genomic DNA fragment of about 3.0 kb.

Sequence analysis of the genomic DNA insert of pZErO-S9 Lib1

Bioinformatics analysis of DNA and protein sequences have been carried out in accordance with the methodology presented in our previous article (Wierzbicka-Wos *et al.*, 2013).

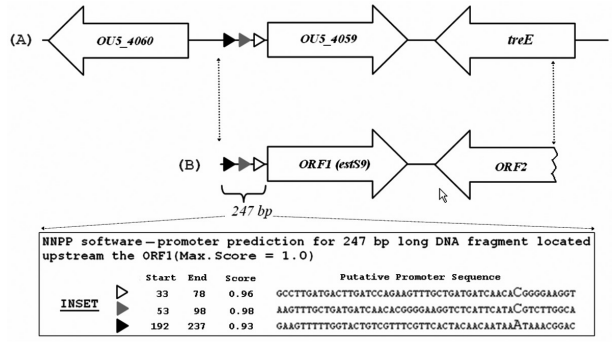

Figure 3. The presence of open reading frames (ORFs) in the genomic insert of *Pseudomonas* sp. S9 (A) and how they correspond with the arrangement of the homologous genes on *Pseudomonas mandelii* JR-1 (B).
INSET — result of *in silica* prediction of sequences of putative promoters for 247 bp long DNA fragment located upstream the OU5_4059 (**A**) and the ORF1 (**B**), respectively

The nucleotide sequence analysis revealed that the DNA insert of the pZErO-S9 Lib1/NotI plasmid contained a complete ORF1 at the 5' terminal, and a partial ORF2 at the 3' terminal (Fig. 3). The complete ORF1 and the partial ORF2 had the highest sequence homology to the DNA sequences of the *OU5_4059* and *treE* genes from the cold-adapted *Pseudomonas mandelii* JR-1, respectively (Jang *et al.*, 2012). In the light of the data deposited in the Genbank database, the *OU5_4059* and *treE* genes encoded a putative outer membrane autotransporter barrel (GenBank: AHZ71138.1) and a putative anthranilate synthase component I (GenBank: AHZ71137.1), respectively. However, more importantly for this study, the product of translation *in silico* of the ORF1 showed high sequence similarity with many putative lipolytic enzymes belonging to α/β hydrolases whose sequences are deposited in the Protein database at National Center for Biotechnology Information (USA).

On the other hand, the layout of the ORFs from the *Pseudomonas* sp. S9 genomic DNA insert (Fig. 3) corresponds to the layout of the *OU5_4059* and *treE* genes in the genome of *Pseudomonas mandelii* JR-1 (NCBI reference sequence: NZ_AJFM00000000.1). Interestingly, orientation of the neighboring genes to the *OU5_4059* gene on the genome of *Ps. mandelii* JR-1 suggests that this gene is expressed from its own promoter. Unfortunately, the analysis of a ~3 kb long genomic DNA insert of *Pseudomonas* sp. S9 from the pZErO-S9 Lib1/NotI plasmid did not confirm the presence of any other ORFs upstream of ORF1. However, the alignment of a 247 bp long DNA fragment located upstream of the ORF1 revealed DNA identities of 97% with a 247 bp long DNA fragment located upstream of the *OU5_4059* gene. This observation led us to analyze both highly conserved DNA fragments using two on-line tools dedicated for prediction of putative promoter sequences. The analysis of both DNA fragments using the NNPP software revealed three highly conserved putative promoter sequences located at the same place in the analyzed DNA fragments (see Inset, Fig. 3). Interestingly, the alternative analysis of both DNA fragments using BProm program revealed only the presence of one putative promoter but with an identical DNA sequence and location as the third putative promoter predicted with NNPP software (black triangle at Inset; Fig. 3). For this reason, it appears

highly possible that the gene encoding the lipolytic enzyme corresponding to ORF1 was expressed from its own promoter in the cells of the *E. coli*/S9_Lib1 clone and *E. coli*/S9_Lib1_NotI clone, respectively.

As mentioned above, the result of the tblastx search revealed that the protein encoded by ORF1 shared the highest sequence identity (97%) with protein annotated not as a putative lipolytic enzyme, but as a putative outer membrane autotransporter barrel in *Pseudomonas mandelii* JR-1 (Jang *et al.*, 2012). However, further detailed analysis of this result revealed that this protein also shared a high sequence identity (91%) with a cold-adapted and biochemically characterized PsEst1 esterase from *Pseudomonas* sp. strain B11-1 (GenBank No.: BAC21259) (Suzuki *et al.*, 2003). Hence, we hypothesized that the ORF1, named *estS9* gene, encoded a putative cold-active and esterolytic enzyme of *Pseudomonas* sp. S9.

The deduced product of the *estS9* gene consisted of 636 amino acid residues with a calculated molecular mass of 68,739 Da. Analysis of the amino acid sequence of EstS9 with InterProScan 5 and CD-search revealed that this protein is composed of two putative domains: a SGNH hydrolase-type esterase/lipase domain (~29–320) and an autotransporter beta domain (~360–626). Moreover, the analysis also revealed the presence of a putative signal peptide of EstS9 enzyme (1–19) which may be involved in EstA transport to the periplasmic space of the host cell (Fig. 1). The detailed sequence analysis of the SGNH hydrolase-type domain of EstS9 revealed that the enzyme contains a canonical putative catalytic triad that would be formed by residues: Ser^{38}, Asp^{162} and His^{303}. Importantly, in contrast to more well-characterized cold-active esterases which contain a catalytic serine residue arranged within the consensus sequence G-X-S-X-G (Suzuki *et al.*, 2002; Kulakova *et al.*, 2004; Soror *et al.*, 2007; Heath *et al.*, 2009; Fu *et al.*, 2011; Kang *et al.*, 2011; Brault *et al.*, 2012; Jiang *et al.*, 2012; Jimenez *et al.*, 2012; Lemak *et al.*, 2012; Novototskaya-Vlasova *et al.*, 2012; Abdul Salam *et al.*, 2013; Berlemont *et al.*, 2013; Fu *et al.*, 2013; Kim *et al.*, 2014), the catalytic serine residue of EstS9 (Ser^{38}) is part of another conserved sequence motif, G-D-S-L. More importantly, this sequence motif is characteristic of the GDSL subfamily of lipolytic enzymes. An important differentiating feature of the GDSL subfamily of lipolytic enzymes is that the sequence motif containing the catalytic serine residue is closer to the N-terminus, unlike other lipases and esterases, where the GXSXG motif is close to the center of the enzyme's sequence (Akoh *et al.*, 2004). To date, to the best of our knowledge, only two other cold-active esterases belonging to the GDSL subfamily, i.e. EstA esterase (~23 kDa) from *Pseudoalteromonas* sp. 643A (Cieslinski *et al.*, 2007) and PsEst1 esterase (~70 kDa) from *Pseudomonas* sp. strain B11-1 (Suzuki *et al.*, 2003), were isolated and characterized. As discussed above, the PsEst1 enzyme shares a high sequence similarity with the EstS9 enzyme. This enzyme also consists of an N-terminal SGNH hydrolase-type domain and a C-terminal autotransporter beta domain (Fig. 1). The presence of the C-terminal AB-domain in EstS9 and PsEst1 suggests that both enzymes may be secreted by the type V secretion system (Henderson *et al.*, 2004).

However, we could not identify any literature data which could confirm this hypothesis for PsEst1. Moreover, it is worthy to note that *the presence of an AB*-domain in the PsEst1 enzyme was not reported in the source article (Suzuki *et al.*, 2003). For comparison, the EstA esterase from *Pseudoalteromonas* sp. strain 643A is secreted by the type I secretion system (Dlugolecka *et al.*, 2008), and characterized by its lack of a C-terminal AB-domain (Brzuszkiewicz *et al.*, 2009).

Our literature search also revealed that the catalytically active N-terminal domain of enzymes secreted by the type V secretion mechanism (i) remains attached to the outer membrane, (ii) is autoproteolytically cleaved off, or (iii) is cleaved off by another protease (Henderson *et al.*, 1998).

Hence, we hypothesized that the mature form of EstS9 may only be composed of a catalytic domain (EstS9 is secreted outside the bacterial cell) or be composed of a catalytic domain and an AB-domain (EstS9 is anchored in the outer membrane and its catalytic domain is present outside the cell). For this reason, in this study, we decided to characterize and compare the biochemical properties of two recombinant forms of the EstS9 protein. The first one, called EstS9N, consists of an N-terminal catalytic domain and a C-terminal AB-domain. The second protein, called EstS9Δ, is characterized by the lack of a C-terminal AB-domain, and its amino acid sequence was designed based on the analysis of InterProScan results. Moreover, in both recombinant proteins, the putative signal peptide was removed. Also, a six-histidine tag (His-tag) was added to the C-terminus of both the EstS9N and EstS9Δ proteins to facilitate purification.

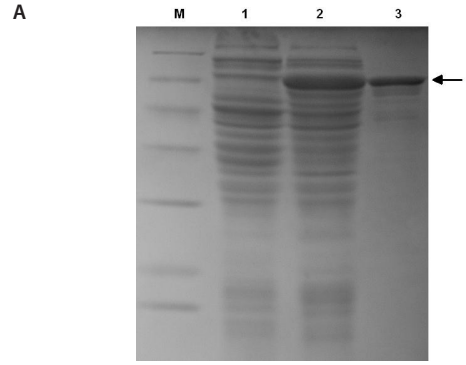

Figure 4A. SDS-PAGE protein profiles: (M) Unstained Protein Molecular Weight Marker 116, 66.2, 45, 35, 25, 18.4, 14.4 kDa (Thermo Scientific, USA), (1) Cell-free extract of *E. coli* TOP10/pBADestS9N, (2) Cell extract of *E. coli* TOP10/pBADestS9N after solubilization of inclusion bodies (3) Purified EstS9N after renaturation

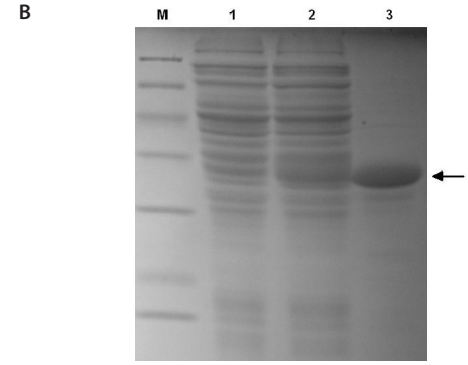

Figure 4B. SDS-PAGE protein profiles: (M) Unstained Protein Molecular Weight Marker 116, 66.2, 45, 35, 25, 18.4, 14.4 kDa (Thermo Scientific, USA), (1) Cell-free extract of *E. coli* TOP10/pBADestS9Δ, (2) Cell extract of *E. coli* TOP10/pBADestS9Δ after solubilization of inclusion bodies, (3) Purified EstS9Δ after renaturation

Table 1. Relative activity of purified EstS9N enzyme with various nitrophenyl-derived chromogenic substrates

Substrate	No. of C atoms in alkyl chain	Relative activity [%]
p-nitrophenyl acetate	2	53 ± 5.1
p-nitrophenyl butyrate	4	100 ± 2.5
p-nitrophenyl caprylate	8	15.5 ± 1.9
p-nitrophenyl caproate	10	6.9 ± 0.8
p-nitrophenyl palmitate	16	< 0.01
p-nitrophenyl stearate	18	< 0.01

Expression and purification of the EstS9N and EstS9Δ proteins

The arabinose-inducible promoter of the pBAD/Myc-His A plasmid was used for the expression of the *estS9N* and *estS9⊿* genes in *E. coli* TOP10 cells. The highest EstS9N and EstS9Δ enzyme production yields were achieved by adding L-arabinose to a final concentration of 0.2% w/v at $OD_{600} = 0.5$ and by extending the cultivation at 30ºC for 20 h. The SDS-PAGE analysis of the *E. coli* cell lysates and cell debris revealed that both recombinant proteins were produced as inclusion bodies. As a result of this, both proteins were purified on a His-Trap affinity column under denaturating conditions and then renatured from urea. Interestingly, both PsEst1 esterase (Suzuki *et al.*, 2003) and EstA esterase (Cieslinski *et al.*, 2007; Dlugolecka *et al.*, 2009) were also produced as inclusion bodies in *E. coli* and then purified under denaturating conditions. SDS-PAGE analysis of the eluted fraction showed distinct protein bands at ~66 kDa and ~35 kDa, which are close to the predicted mass of the deduced EstS9N and EstS9Δ proteins with the addition of a six-histidine tag, respectively (Fig. 4A and 4B). Preliminary experiments showed that *p*-nitrophenyl butyrate was hydrolyzed by both, the purified and renatured proteins. Moreover, the concentration of purified EstS9Δ (1.25 mg mL^{-1}) was two times higher than the concentration of purified EstS9N (0.58 mg mL^{-1}), however, the EstS9Δ enzyme had only ~3% of the specific enzymatic activity and ~6% of the total enzymatic activity of EstS9N, respectively ($EstS9N_{spec.act.} = 0.088$ U mg^{-1}; $EstS9N_{total.act.} = 0.77$ U; $EstS9\Delta_{spec.act.} = 0.0025$ U mg^{-1}; $EstS9\Delta_{total.act.} = 0.046$ U). Therefore, we decided to only characterize the EstS9N enzyme further.

Substrate specificity, physicochemical characterization and determination of kinetic parameters of EstS9N

Substrate specificity of EstS9N esterase was investigated using *p*-nitrophenyl esters of different alkyl chain lengths. As it is shown in Table 1, the EstS9N enzyme had a high activity towards short chain fatty acids (C2–C8), and exerted the maximum activity against the *p*-nitrophenyl butyrate ester. Importantly, the comparative analysis of results of *p*-nitrophenyl esters' hydrolysis by PsEst1 (Suzuki *et al.*, 2003) and EstS9N enzymes revealed the distinct differences in substrate specificity for both compared enzymes. In contrast to PsEst1, the EstS9N enzyme showed a higher activity against *p*-nitrophenyl acetate and a lower activity against *p*-nitrophenyl caproate and caprylate, respectively.

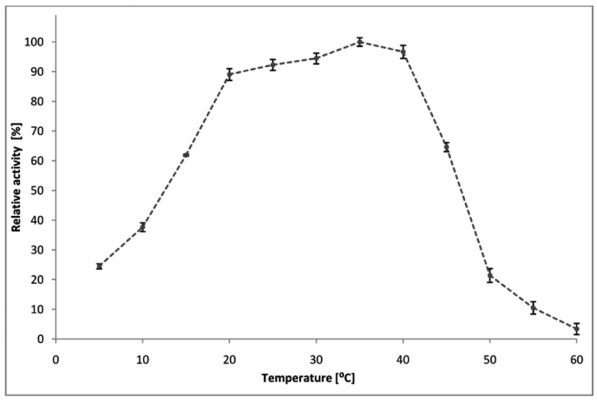

Figure 5. The effect of temperature on the recombinant EstS9N enzyme activity
The effect of temperature on the esterase activity was assayed by incubating the EstS9N enzyme (9 min) at a temperature ranging from 5 to 60ºC (at 5ºC increments) with *p*-nitrophenyl butyrate at a final concentration of 3.6 mM, in 20 mM Tris-HCl buffer, pH 7.5.

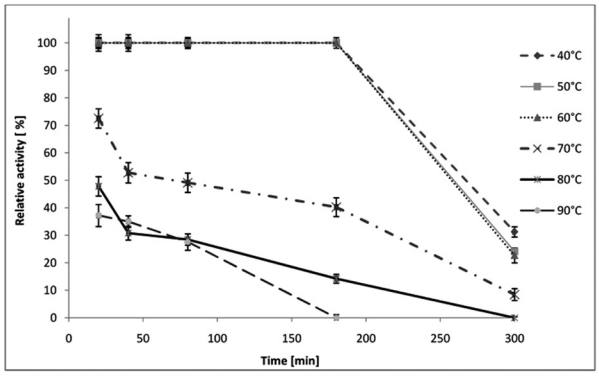

Figure 6. The effect of temperature on the recombinant EstS9N esterase stability
The purified enzyme was pre-incubated at 40, 50, 60, 70, 80 and 90°C in the absence of *p*-nitrophenyl butyrate, respectively. After incubation for different times (20, 40, 80, 180 and 300 min), the residual activity of the enzyme was assayed under standard conditions (9 min incubation at 25°C, pH 9.0).

The optimal temperature for the esterase activity of EstS9N was determined from 5 to 60°C. As shown in Fig. 5, the maximum activity was at 35°C, but the enzyme retained ~90% of its activity in the range of 25-40°C and ~40% of its activity at 10°C. By comparison, the thermal optimum of PsEst1 is 45°C. Moreover, 100% of the EstS9N enzyme activity was retained after 3 h of incubation over a temperature range of 40 to 60°C, and the enzyme was gradually inactivated by heat treatment at temperatures above 70°C (Fig. 6). The thermostability of the EstS9N enzyme was significantly higher than PsEst1 (Suzuki *et al.*, 2003).

The optimal pH for the esterase activity of EstS9N was determined over a pH range of 2.0 to 12.0, at 25°C. As shown in Fig. 7, the enzyme was active over a pH range of 5.5 to 10.5 and preferred alkaline conditions with an optimum activity at pH 9.0. The results from the pH stability assay showed that ~100% of the enzyme activity was retained at the optimal pH, however, at pH 8 and pH 10, the enzyme was gradually inactivated (Fig. 8). In contrast to the EstS9N esterase, the PsEst1 enzyme was stable under acidic and alkaline conditions (Suzuki *et al.*, 2003).

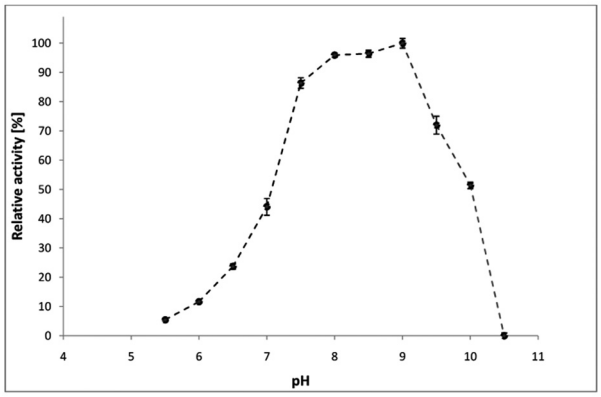

Figure 7. The effect of pH on the recombinant EstS9N enzyme activity
The enzymatic activity was assayed at the tested pH values (from pH 2.0 to 12.0), at 25°C, with *p*-nitrophenyl butyrate as a substrate.

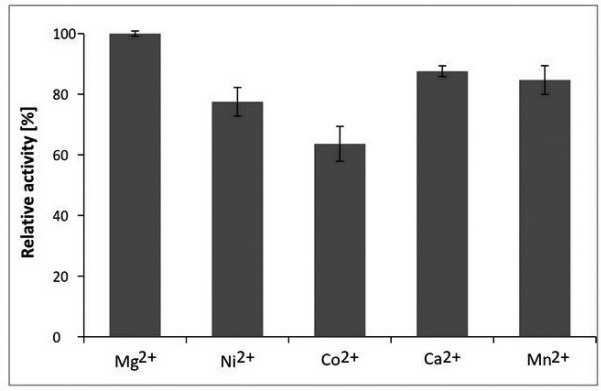

Figure 9. The effect of various metal ions on EstS9N esterase activity
The enzyme was incubated for 60 min at 25°C with 5 mM metal ions, and then the residual activity of enzyme was assayed under standard conditions.

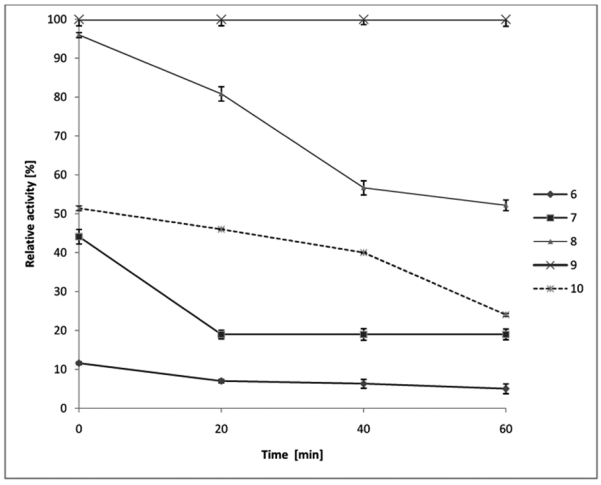

Figure 8. The effect of pH on the recombinant EstS9N esterase stability
pH-stability was determined by incubation of the esterase for 0, 20, 40 and 60 min at various pH, and then the residual activity of enzyme was assayed under standard conditions.

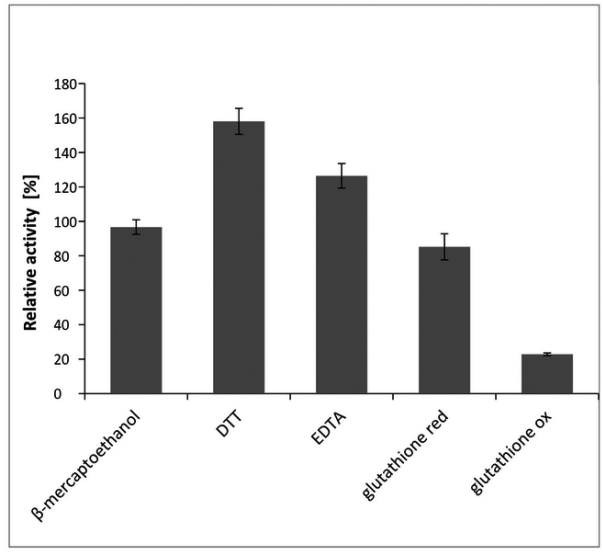

Figure 10. The effect of selected reagents on EstS9N esterase activity
The enzyme was incubated for 60 min at 25°C with 5 mM of β-mercaptoethanol, DTT, EDTA, glutathione in reduced and oxidized states, and then the residual activity of enzyme was assayed under standard conditions.

A study of its kinetic properties (K_m, k_{cat} and k_{cat}/K_m) revealed that EstS9N had lower affinities (K_m values) for *p*-nitrophenyl butyrate at the optimum temperature of enzymatic activity (35°C) than at lower temperatures (15°C and 25°C). Moreover, as shown in Table 2, the k_{cat}/K_m values for *p*-nitrophenyl butyrate at 25°C and 15°C, are approximately 12 and 2 times higher than the k_{cat}/K_m value at the optimum temperature of enzymatic activity. In summary, the EstS9N enzyme has the highest enzymatic efficiency known at a temperature close to the growth optimum for *Pseudomonas* sp. S9 (20°C).

Table 2. Kinetic parameters of EstS9N
The enzyme was incubated at 15, 25 or 35°C with p-nitrophenyl butyrate at a final concentration of 3.6 mM, in 20 mM Tris-HCl buffer, pH 7.5. The enzymatic reaction was stopped after 9 min with isopropanol.

Temperature [°C]	K_m [mM]	k_{cat} [s^{-1}]	k_{cat}/K_m [s^{-1} mM^{-1}]
15	0.0368	1.45	39.50
25	0.0095	2.39	252.22
35	0.1617	3.31	20.48

As shown in Fig. 9, the hydrolytic activity of EstS9N against *p*-nitrophenyl butyrate as a substrate, was clearly inhibited by Ni^{2+}, Co^{2+}, Ca^{2+}, and Mn^{2+} ions. We also observed that the addition of EDTA to freshly purified enzyme markedly increased its enzymatic activity (Fig. 10). Hence, it seems to be highly possible that EDTA chelated the Ni^{2+} ions which were co-eluted with the enzyme during its purification on the Ni-NTA column helping to restore the enzyme activity.

The Cys residues are not directly involved in the catalysis of the hydrolysis reaction catalyzed by lipolytic enzymes belonging to the GDSL subfamily. However, the presence of two putative disulfide bonds (predicted with the DiANNA 1.1 program), which could be present in native enzyme or could be formed during

refolding process, encouraged us to check the effect of selected reducing or oxidizing agents on enzymatic activity of EstS9 esterase. As shown in Fig. 10, dithiothreitol (reducing agent) significantly increased the enzyme activity, whereas oxidized glutathione (oxidizing agent) significantly decreased its activity. Hence, we hypothesized that the positive effect of the DTT on the EstS9N enzymatic activity may be a result of the reduction of an intramolecular and/or intermolecular disulfide bond (or bonds) between the cysteine residues of the analyzed enzyme, which could be formed during enzyme production and/or purification. β-Mercaptoethanol and glutathione (reduced form), two other reducing agents, did not have an effect on the enzyme activity. However, it may be possible that these compounds could not reduce the putative disulfide bonds formed in EstS9N because these are weaker reducing agents than dithiothreitol.

CONCLUSION

Although there is a significant knowledge about cold active esterases belonging to GXSXG subfamily, the data available on the cold active esterases belonging to GDSL subfamily is very poor. In this study, we identified, isolated and partially characterized two recombinant variants of EstS9, a putative cold active esterase belonging to GDSL subfamily. The results of the study confirmed that both recombinant variants of EstS9 protein have esterase activity. Moreover, the study on EstS9N kinetic properties showed that this recombinant variant of EstS9 enzyme is a cold active esterase.

On the other hand, despite the fact that the yield of the purified EstS9Δ enzyme was remarkably higher than that for the purified EstS9N, its enzymatic activity was also much lower than EstS9N. Hence, taking into account that the EstS9 enzyme could be secreted by the type V secretion mechanism, we hypothesized that the obtained results may suggest that the mature form of the native EstS9 enzyme is composed of two domains. Evidence for this hypothesis was supported by the results of Wilhelm and coworkers who reported that the mature form of EstA esterase, isolated from mesophilic *Pseudomonas aureginosa* strain PAO1, is located in the outer membrane of the host cell and is composed of an N-terminal catalytic domain and a C-terminal autotransporter domain (Wilhelm *et al.*, 1999). Therefore, our future work will include production and characterization of the native EstS9 enzyme. Additionally, we plan to build on the esterolytic activity of the EstS9Δ enzyme by employing an *in vitro* directed molecular evolution for the generation of EstS9Δ-derivatives for selection of a stable and efficient biocatalyst. If this approach proves successful, the selected EstS9Δ-derivative will be enzymatically characterized and its biotechnological potential will be evaluated.

REFERENCES

Abdul Salam J, Lakshmi V, Das D, Das N (2013) Biodegradation of lindane using a novel yeast strain, *Rhodotorula* sp. VITJzN03 isolated from agricultural soil. *World J Microb Biotechol* **29**: 475–87. doi: 10.1007/s11274-012-1201-4.

Akoh CC, Lee GC, Liaw YC, Huang TH, Shaw JF (2004) GDSL family of serine esterases/lipases. *Prog Lipid Res* **43**: 534–552. doi: 10.1016/j.plipres.2004.09.002.

Arpigny JL, Jaeger KE (1999) Bacterial lipolytic enzymes: classification and properties. *Biochem J* **343**: 177–83. doi: 10.1042/0264-6021:3430177.

Berlemont R, Jacquin O, Delsaute M, La Salla M, Georis J, Verte F, Galleni M, Power P (2013) Novel cold-adapted esterase mhlip from an antarctic soil metagenome. *Biology* **2**: 177–188. doi:10.3390/biology2010177.

Brault G, Shareck F, Hurtubise Y, Lepine F, Doucet N (2012) Isolation and characterization of EstC, a new cold-active esterase from *Streptomyces coelicolor* A3(2). *PloS one* **7**: e32041. doi: 10.1371/journal.pone.0032041.

Brzuszkiewicz A, Nowak E, Dauter Z, Dauter M, Cieslinski H, Dlugolecka A, Kur J (2009) Structure of EstA esterase from psychrotrophic *Pseudoalteromonas* sp 643A covalently inhibited by monoethylphosphonate. *Acta Crystallogr F* **65**: 862–865. doi: 10.1107/S1744309109030826.

Cavicchioli R, Charlton T, Ertan H, Mohd Omar S, Siddiqui KS, Williams TJ (2011) Biotechnological uses of enzymes from psychrophiles. *Microb Biotechnol* **4**: 449–460. doi: 10.1111/j.1751-7915.2011.00258.x.

Cieslinski H, Bialkowska AM, Dlugolecka A, Daroch M, Tkaczuk KL, Kalinowska H, Kur J, Turkiewicz M (2007) A cold-adapted esterase from psychrotrophic *Pseudoalteromas* sp strain 643A. *Arch Microbiol* **188**: 27–36. doi: 10.1007/s00203-007-0220-2.

Dlugolecka A, Cieslinski H, Bruzdziak P, Gottfried K, Turkiewicz M, Kur J (2009) Purification and biochemical characteristic of a cold-active recombinant esterase from *Pseudoalteromonas* sp 643A under denaturing conditions. *Pol J Microbiol* **58**: 211–218.

Dlugolecka A, Cieslinski H, Turkiewicz M, Bialkowska AM, Kur J (2008) Extracellular secretion of *Pseudoalteromonas* sp cold-adapted esterase in *Escherichia coli* in the presence of *Pseudoalteromonas* sp components of ABC transport system. *Protein Expres Purif* **62**: 179–184. doi: 10.1016/j.pep.2008.07.006.

Esteban-Torres M, Mancheno JM, de las Rivas B, Munoz R (2014) Characterization of a cold-active esterase from *Lactobacillus plantarum* suitable for food fermentations. *J Agr Food Chem* **62**: 5126–5132. doi: 10.1021/jf501493z.

Fojan P, Jonson PH, Petersen MT, Petersen SB (2000) What distinguishes an esterase from a lipase: a novel structural approach. *Biochimie* **82**: 1033–1041. doi: 10.1016/S0300-9084(00)01188-3.

Fu J, Leiros HKS, de Pascale D, Johnson KA, Blencke HM, Landfald B (2013) Functional and structural studies of a novel cold-adapted esterase from an Arctic intertidal metagenomic library. *Appl Microbiol Biot* **97**: 3965–3978. doi: 10.1007/s00253-012-4276-9.

Fu C, Hu Y, Xie F, Guo H, Ashforth EJ, Polyak SW, Zhu B, Zhang L (2011) Molecular cloning and characterization of a new cold-active esterase from a deep-sea metagenomic library. *Appl Microbiol Biotechnol* **90**: 961–970. doi: 10.1007/s00253-010-3079-0.

Heath C, Hu XP, Cary SC, Cowan D (2009) Identification of a novel alkaliphilic esterase active at low temperatures by screening a metagenomic library from antarctic desert soil. *Appl Environ Microb* **75**: 4657–4659. doi: 10.1128/AEM.02597-08.

Henderson IR, Navarro-Garcia F, Desvaux M, Fernandez RC, Ala'Aldeen D (2004) Type V protein secretion pathway: the autotransporter story. *Microbiol Mol Biol R* **68**: 692–744. doi:10.1016/s0966-842x(98)01318-3.

Henderson IR, Navarro-Garcia F, Nataro JP (1998) The great escape: structure and function of the autotransporter proteins. *Trends Microbiol* **6**: 370–378. doi:10.1016/s0966-842x(98)01318-3.

Hu XP, Heath C, Taylor MP, Tuffin M, Cowan D (2012) A novel, extremely alkaliphilic and cold-active esterase from Antarctic desert soil. *Extremophiles* **16**: 79–86. doi: 10.1007/s00792-011-0407-y.

Jang SH, Kim J, Kim J, Hong S, Lee C (2012) Genome sequence of cold-adapted *Pseudomonas mandelii* strain JR-1. *J Bacteriol* **194**: 3263–3263. doi: 10.1128/JB.00517-12.

Jiang X, Xu X, Huo Y, Wu Y, Zhu X, Zhang X, Wu M (2012) Identification and characterization of novel esterases from a deep-sea sediment metagenome *Arch Microbiol* **194**: 207–214. doi: 10.1007/s00203-011-0745-2.

Jimenez DJ, Montana JS, Alvarez D, Baena S (2012) A novel cold active esterase derived from Colombian high Andean forest soil metagenome. *World J Microb Biot* **28**: 361–70. doi: 10.1007/s11274-011-0828-x.

Kang CH, Oh KH, Lee MH, Oh TK, Kim BH, Yoon J (2011) A novel family VII esterase with industrial potential from compost metagenomic library. *Microb Cell Fact* **10**: 41. doi: 10.1186/1475-2859-10-41.

Kim YO, Park IS, Nam BH, Kim DG, Jee YJ, Lee SJ, An CM (2014) A novel esterase from *Paenibacillus* sp. PBS-2 is a new member of the beta-lactamase belonging to the family VIII lipases/esterases. *J Microbiol Biotechn* **24**: 1260–1268.

Kulakova L, Galkin A, Nakayama T, Nishino T, Esaki N (2004) Cold-active esterase from *Psychrobacter* sp. Ant300: gene cloning, characterization, and the effects of Gly-->Pro substitution near the active site on its catalytic activity and stability. *Biochim Biophys Acta,* **1696**: 59–65. doi: 10.1016/j.bbapap.2003.09.008.

Laemmli UK (1970) Cleavage of Structural Proteins during Assembly of Head of Bacteriophage-T4. *Nature* **227**: 680–685. doi: 10.1038/227680a0.

Lemak S, Tchigvintsev A, Petit P, Flick R, Singer AU, Brown G, Evdokimova E, Egorova O, Gonzalez CF, Chernikova TN, Yakimov MM, Kube M, Reinhardt R, Golyshin PN, Savchenko A, Yakunin AF (2012) Structure and activity of the cold-active and anion-activated carboxyl esterase OLEI01171 from the oil-degrading marine bacterium *Oleispira antarctica*. *Biochem J* **445**: 193–203. doi: 10.1042/BJ20112113.

Novototskaya-Vlasova K, Petrovskaya L, Yakimov S, Gilichinsky D (2012) Cloning, purification, and characterization of a cold-adapted esterase produced by *Psychrobacter cryohalolentis* K5T from Siberian cryopeg. *Fems Microbiol Ecol* **82**: 367–375. doi: 10.1111/j.1574-6941.2012.01385.x.

Reddy PVV, Rao SSSN, Pratibha MS, Sailaja B, Kavya B, Manorama RR, Singh SM, Srinivas TNR, Shivaji S (2009) Bacterial diversity and bioprospecting for cold-active enzymes from culturable bacteria associated with sediment from a melt water stream of Midtre Lovenbreen glacier, an Arctic glacier. *Res Microbiol* **160**: 538–546. doi: 10.1016/j.resmic.2009.08.008.

Soror SH, Verma V, Rao R, Rasool S, Koul S, Qazi GN, Cullum J (2007) A cold-active esterase of *Streptomyces coelicolor* A3(2): from genome sequence to enzyme activity. *J Ind Microbiol Biot* **34**: 525–531. doi: 10.1007/s10295-007-0224-6.

Suzuki T, Nakayama T, Choo DW, Hirano Y, Kurihara T, Nishino T, Esaki N (2003) Cloning, heterologous expression, renaturation, and characterization of a cold-adapted esterase with unique primary structure from a psychrotroph *Pseudomonas* sp. strain B11-1. *Protein Expres Purif* **30**: 171–178. doi: 10.1016/S1046-5928(03)00128-1.

Suzuki T, Nakayama T, Kurihara T, Nishino T, Esaki N (2002) Primary structure and catalytic properties of a cold-active esterase from a psychrotroph, *Acinetobacter* sp. strain No. 6. isolated from Siberian soil. *Biosci Biotech Bioch* **66**: 1682–1690. doi: 10.1271/bbb.66.1682.

Weisburg WG, Barns SM, Pelletier DA, Lane DJ (1991) 16S ribosomal DNA amplification for phylogenetic study. *J Bacteriol* **173**: 697–703.

Wierzbicka-Wos A, Bartasun P, Cieslinski H, Kur J (2013) Cloning and characterization of a novel cold-active glycoside hydrolase family 1 enzyme with beta-glucosidase, beta-fucosidase and beta-galactosidase activities. *BMC Biotechnol* **13**: 22. doi: 10.1186/1472-6750-13-22.

Wilhelm S, Tommassen J, Jaeger KE (1999) A novel lipolytic enzyme located in the outer membrane of *Pseudomonas aeruginosa*. *J Bacteriol* **181**: 6977–6986.